Title

The developmental long trace profiler (DLTP) optimized for metrology of side-facing optics at the ALS

ISBN

9781628412338

Authors

Lacey, Ian
Artemiev, Nikolay A
Domning, Edward E
et al.

Publication Date

2014-09-17

DOI

10.1117/12.2061969

Peer reviewed

The developmental long trace profiler (DLTP) optimized for metrology of side-facing optics at the ALS

Ian Lacey, Nikolay Artemiev, Edward Domning, Wayne McKinney, Gregory Morrison, et al.

Ian Lacey, Nikolay A. Artemiev, Edward E. Domning, Wayne R. McKinney, Gregory Y. Morrison, Simon A. Morton, Brian V. Smith, Valeriy V. Yashchuk, "The developmental long trace profiler (DLTP) optimized for metrology of side-facing optics at the ALS," Proc. SPIE 9206, Advances in Metrology for X-Ray and EUV Optics V, 920603 (17 September 2014); doi: 10.1117/12.2061969

SPIE.

Event: SPIE Optical Engineering + Applications, 2014, San Diego, California, United States

The developmental long trace profiler (DLTP) optimized for metrology of side-facing optics at the ALS

Ian Lacey*, Nikolay A. Artemiev, Edward E. Domning, Wayne R. McKinney, Gregory Y. Morrison, Simon A. Morton, Brian V. Smith, and Valeriy, V, Yashchuk
Lawrence Berkeley, National Laboratory, Berkeley, CA USA 94720

ABSTRACT

The autocollimator and moveable pentaprism based DLTP [NIM A 616 (2010) 212-223], a low-budget, NOM-like profiler at the Advanced Light Source (ALS), has been upgraded to provide fast, highly accurate surface slope metrology for long, side-facing, x-ray optics. This instrument arrangement decreases sensitivity to environmental conditions and removes the gravity effect on mirror shape. We provide design details of an affordable base tool, including clean-room environmental arrangements in the new ALS X-ray Optics Laboratory with advanced temperature stabilization and turbulence reduction, that yield measurements in under 8 hours with accuracy better than 30 nanoradians (rms) for super polished,190 mm flat optics, limited mainly by residual temporal instability of the experimental set-up. The upgraded DLTP has been calibrated for highly curved x-ray optics, allowing same day measurements of a 15 m ROC sphere with accuracy of better than 100 nanoradians (rms). The developed calibration procedure is discussed in detail. We propose this specific 15 m ROC sphere for use as a round-robin calibration test optic.

Keywords: Surface Metrology, long trace profiler, surface slope measurement, x-ray optics, large measurement range, accuracy, stability, nanoradian repeatability, synchrotron radiation.

1. INTRODUCTION

Development of X-ray optics for 3rd and 4th generation X-ray light sources and x-ray free electron lasers (XFELs) with a level of surface slope precision better than 150 nrad requires the development of adequate fabrication technologies and associated dedicated metrology instrumentation and methods.[1,2]

The best performing slope measuring profilers, such as the Nanometer Optical Component Measuring Machine (NOM) at Helmholtz Zentrum Berlin (HZB)/BESSY-II (Germany),[3-6] the Developmental Long Trace Profiler (DLTP) at the Advanced Light Source (ALS),[10] and the Extended Shear Angle Difference (ESAD) instrument at the PTB (Germany), [7-9] come close to the required precision. These instruments utilize a schematic with a movable pentaprism[10-14] and an electronic autocollimator (AC) as a non-contact slope sensor.[3,15] The high performance of the instruments is based on the precision calibration of the ACs for the specific application with aperture diameters in the range of 2.5 - 5 mm.[16-18]

The ALS DLTP was brought into operation in 2009 for surface slope metrology of face-up optics.[10] Similar to the NOM and ESAD, the DLTP is based on a movable pentaprism and a precision calibrated autocollimator. In contrast to the NOM, this is a low budget instrument originally used at the ALS for the development and testing of new measurement strategies. Some of the methods developed with the DLTP[18-23] have been implemented into the ALS LTP-II slope measuring long trace profiler,[24,25] and are in use with the DLTP for routine metrology with x-ray optics.

Besides the application as a test facility, the DLTP is supplementary to the existing LTP-II. There are a number of arguments for having two principally different instruments that perform the same function. First, the systematic errors of an autocollimator-based instrument are significantly different[24] than that of the LTP. In the LTP, the optical reference arm was added[26] to monitor the carriage wiggling and laser pointing instability. Unfortunately, the current performance of the reference arm is one of the most important factors limiting the accuracy of LTP measurements.[27]

The use of a movable, mirror-based pentaprism in the DLTP[28-30] makes the slope measurement insensitive, in first approximation, to carriage wobble. Second, the use of an autocollimator, precisely calibrated with a high performance stationary calibration system, as the one at the PTB,[16,17] allows transfer of calibration accuracy to the DLTP measurement. Third, the closed and self-sufficient design and high stability of the DLTP autocollimator[31] provides an

* ilacey@lbl.gov

Advances in Metrology for X-Ray and EUV Optics V, edited by Lahsen Assoufid, Haruhiko Ohashi, Anand Krishna Asundi, Proc. of SPIE Vol. 9206, 920603

opportunity for a deep automation of the measurement process[22] that can otherwise require a very long time for adequate suppression of the errors due to instrumental drifts and systematic effects.

In the present work, we describe the recent upgrade and configuration of the DLTP, now operational in the new ALS X-Ray Optics Lab (XROL),[32] optimally arranged to measure side-facing optics. This arrangement both further compliments the capability of LTP-II in the case of side-facing beamline mirror assemblies, and provides highly accurate metrology of bare substrates, otherwise sensitive to gravity. Special attention is paid to precisely calibrate the DLTP for enabling slope metrology of significantly curved optics providing accuracy on the level of 100 nrad rms. The procedure of the calibration is discussed in details.

2. DLTP STABILITYAND PERFORMANCE WITH PLANE OPTICS

Figure 1 shows the new experimental arrangement of the upgraded DLTP in the XROL[32]. Mounted on an 8 ft × 4 ft optical table, the DLTP is surrounded with a hutch and a curtain.

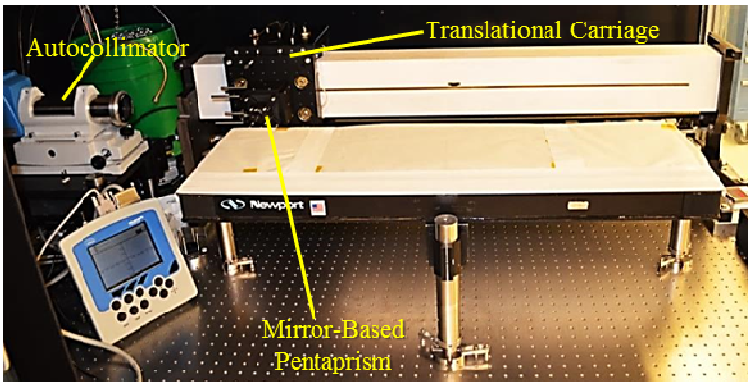

Figure 1: Operational components of the NOM-like instrument, showing the autocollimator, moveable pentaprism, and the transaltional carriage.

For the purpose of establishing the scale to which the hutch and curtains isolate the optical table from environmental room temperature fluctuations, a "signal" was generated by fluctuating the room temperature by 125 mK rms with a period of about four and a half minutes. With this driving signal, we can monitor the temperatrue of the hutch and the temperature of the optical table to understand the effect the curtians and the hutch have respectively on the enclosed instrumentation.[32] While the temperatrue of the aluminum frame of the instrument hutch, insulated only by the plastic curtains, varied by 11 mK rms the optical table exhibited only a 1.4 mK rms temperatrue variation during the 75 minute test.

The compressed air supply to air bearings of the translational carriage is from the ALS house-air. This supply passes into a 200 liter reservoir, then a drier and a set of double filteres before entering the instruemnt hutch. Inside the instrument hutch the air supply passes through a 50 ft coil of copper tubing immersed in a sealed water bath before passing through a pressure regulator just upstream of the carriage bearings. In this way, the air exiting the carriage air bearings will have a minimal impact on the internal temperature of the hutch.

After the inlet air supply was temperature stabalized, the pressure was optimized[33,34] to provide steady support for the weight of the translational stage. With the fine adjustment of the air inlet valve, the rms variation of the air pressure was reduced from 25 mBar to 6 mBar.

2.1 AC-X signal vs. AC-Y signal

To understand the impact on measuremets, the autocollimator readings with a mirror placed on the translational stage, upstream of the pentaprism, are presented in Fig. 2.

While there is an apparent increase in the rms variation of both the Y and X signals for the stability scan using the pentaprism, 150 nrad and 110 nrad respectively, this may be attributed to the longer optical path with the associated residual air convection turbulence, compared to the first stability scan using a mirror mounted directly on the carriage, and in either case the X signal veries roughly 20% less than the Y signal.

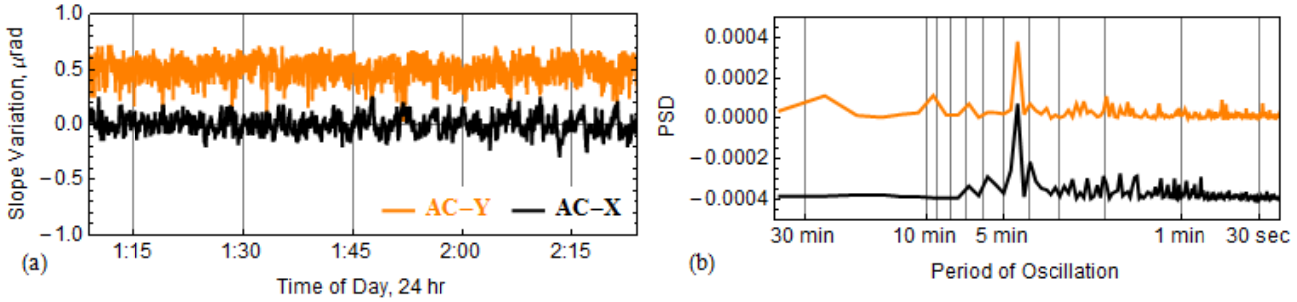

Figure 2: Stability scan with a mirror on the translational carriage, reflecting directly back to the autocollimator, (a) the vertical, AC-Y, and horizontal, AC-X signals recorded for the 75 minute duration of the stability scan, and (b) the associated PSD.

In both channels, the vertical, Y, and the horizontal, X, there remains a periodic fluctuation of the reading with the same frequency as the pressure variation. The rms variation is 100 nrad for the Y direction and 83 nrad for the X direction. For actual measurement runs, when the mirror-based pentaprism is used, the fluctuations of the carriage should be reduced, Fig. 3.

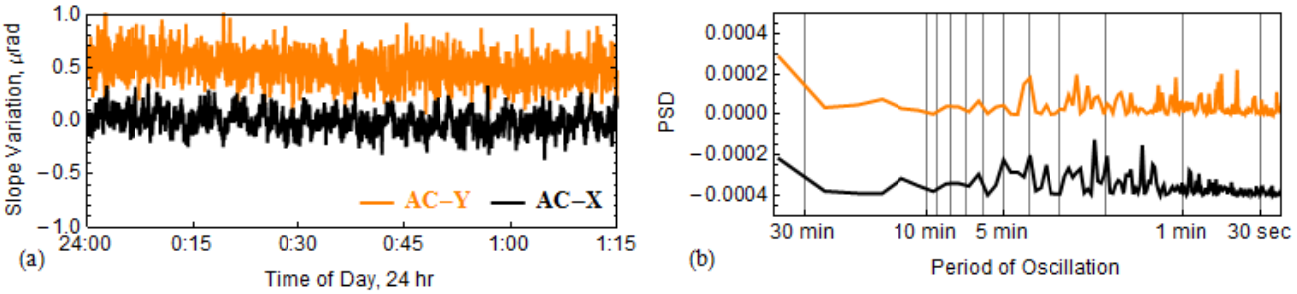

Figure 3: Stability scan of the autocollimator Y and X readings showing angular position of a reference mirror fixed to the optical table (a). The associated PSD showing a reduction of the ~4.5 minute fluctuation present in the compressed air line (b).

2.2 Long-term stability

Together with the improved environmental conditions in the new lab,[28] the hutch and curtain provide extremely stable temperature of the set-up, better than 2 mK rms per day. The stability of the DLTP measurements was tested in a self-test mode of operation of the instrument. In this case, a reference mirror was mounted to the DLTP carriage just in front of the autocollimator. The carriage air-bearings are supplied with pressurized air, but the position of the carriage is steady. The result of the stability tests is shown in Fig. 4.

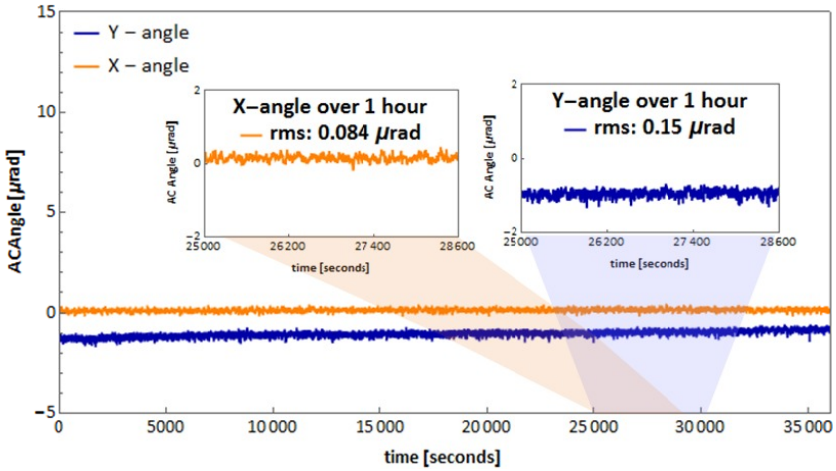

Figure 4: The upgraded DLTP stability test performed during approximatelly 10 hours.

The one hour stability of the X channel of the autocollimator (corresponding to the slope measurement in the tangential direction), with 84 nrad rms variation, is almost twice better than the Y channel of the autocollimator (corresponding to the slope measurement in the sagittal direction) showing a 150 nrad rms variation over the same period. Note that for a standard run of 8 scans performed according to the measurement strategy, optimized for effective suppression of the instrumental drift error up to the third polynomial,[22] the contribution of the instability to the measurement result corresponds to an instability of about 30 nrad and 35 nrad rms, respectively for the X and Y channels. The difference is significantly smaller because of suppression of the larger drift error for the Y-channel.

The stability demonstrated in Fig. 4 corresponds to the repeatability of the upgraded DLTP observed in the measurements with a plane optic, Fig 5. In the course of this test, the DLTP was operated in the normal measurement mode, scanning along the 170 mm clear aperture of a 180 mm long, plane reference mirror.

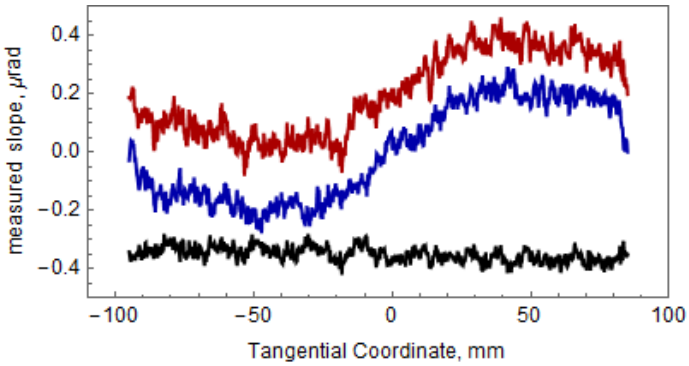

Figure 5: Repeatability of DLTP measurements after optimizing the XROL environmental conditions, including the DLTP compressed air supply. The top two curves are the pair of repeated measurements, and the bottom curve, is the half the difference between the pair with rms variation of 26 nrad, offset added for clarity.

A measure of repeatability is the half difference between repeated pairs of measurements. In this case it was found to be 26 nrad rms. This repeatability test was, itself repeated, with the same 26 nrad result.

3. THE PERFORMANCE OF THE UPGRADED DLTP WITH CURVED OPTICS

The DLTP performance with significantly curved x-ray optics was verified by measuring a 15 m ROC spherical test mirror, the same one that was used in Ref.[10] after initial assembly of the DLTP, then for face-up optics. The strong mirror curvature tests the profiler over the entire dynamic range of the AC, which is ±4.6 mrad. The previous measurements allowed the determination of systematic error of the DLTP measurements with the curve optic to be on the level of nearly 400 nrad. The problem is that the calibration of the AC performed at the PTB[35,36] using the high precision angular comparator, is valid only for a fixed distance[37,38] between the AC and the SUT. Therefore, a special sequence of measurements, with a goal to calibrate the DLTP for the current experimental arrangement, side-facing, that we routinely use for measurements with x-ray optics. Below we discuss the developed calibration procedure and the results of application of the procedure in order to obtain truthful surface slope topography of the 15 m spherical reference.

3.1 Measurement sequence

A series of measurements was performed using a high quality 15 m ROC reference mirror substrate in both the direct and flipped orientation[22] where the substrate was rotated with respect to the zero autocollimator reading at the center of the clear aperture. From these measurements, a calibration file of the instrumental systematic errors was created. This calibration curve can be subtracted from present and prior measurements to give a more accurate slope profile of curved optics under test.

In order to allow surface slope measurements to have vastly different angular ranges compared to the common tangential coordinate range, measurements of the substrate were divided into seven regional traces. For measurements associated with each regional trace, the substrate was tilted so that at the tangential central coordinate of the specific regional trace, the measured angle was nearly zero, schematically shown in Fig 6. A further detail is that each regional trace consists of a pair of measurements, with approximately a 140 µrad tilt between each member of the pair; to compensate for a high

frequency systematic error with a period of 280 μrad[26], where a single measurement consists of eight scans conducted according to the optimal sequence of measurements to reduce drift error.[22]

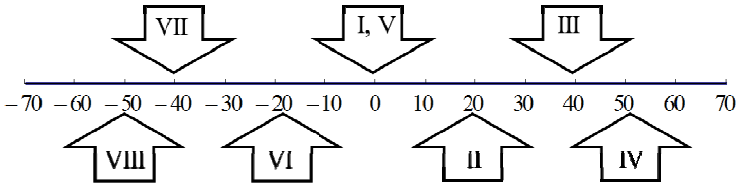

Figure 6: Showing the sequence of regional trace pairs of measurements along the spherical reference mirror, where for each regional trace, the substrate was rotated with respect to the DLTP translational stage to give a zero autocollimator reading at the specified points, 20 mm apart, with the exception of the extreme ends, 20 mm there from.

Successive measurements of the regional trace pairs, I through VIII, were performed in a non-uniform order, with the central region repeated, as means to reduce the impact of slow drift and to track the repeatability. Each sequence of measurements is conducted for both the direct and flipped orientation of the substrate.

Additionally, two more measurement pairs were performed with the substrate translated by 25 mm upstream and 25 mm downstream along the tangential axis to inspect the translational stability of measurements.

3.2 Data processing employed to elucidate systematic errors

The residual slope trace (after subtraction of the best fit sphere), is parsed within the working calibration range of the autocollimator. When considered as a function of the best fit parameter of the subtracted sphere, the residual slopes, as a function of that best linear fit, are combined and averaged over their common angular ranges, Fig. 7. For the determination of a common angle range the calibrated residual slope traces are coordinated by interpolation to the best linear fit function with 5 μrad increments.

This procedure, of working in the angular domain differs from the method proposed by Polack et al.,[39] and acts to reduce the contribution of the actual mirror surface slope from the results, since the common angular range of regional traces is coincident with completely different residual surface topology.

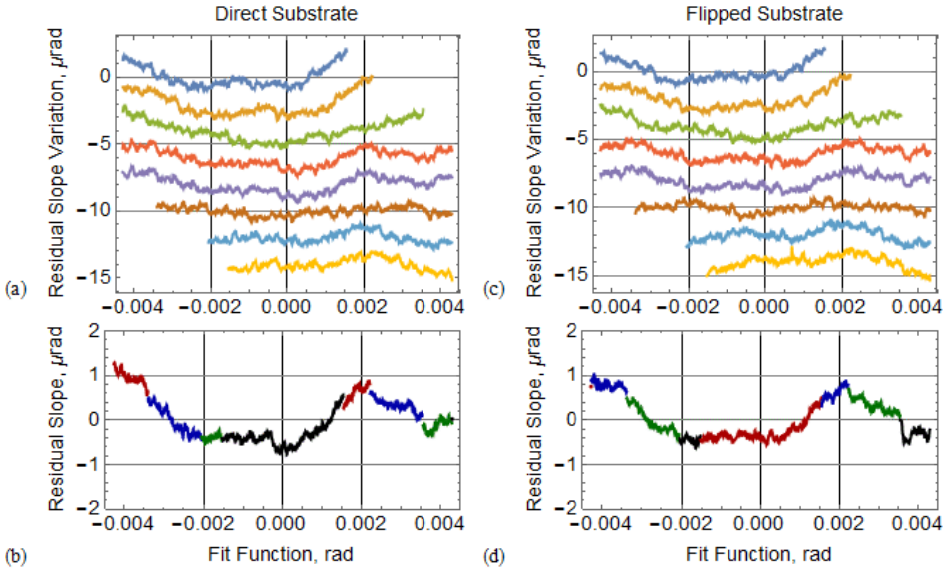

Figure 7: Residual angle as a function of best linear fit of the measured slope, for each regional trace pair of measurements, (a) and (c); offset added for clarity. The average of the regional trace residuals as a function of fit over the common angular domains, (b) and (d).

The average of the residuals as a function of fit, over common angular ranges, for each orientation of the substrate are then averaged together, thus further reducing the contribution of the mirror surface to the obtained results, Fig 8.

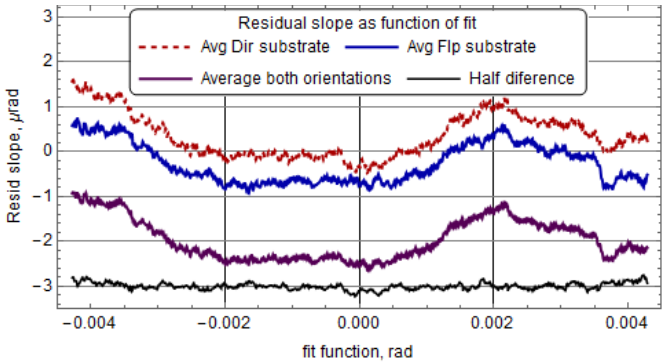

Figure 8: Showing the combined average residuals as a function of fit for each orientation of the substrate, direct and flipped, upper two curves respectively, and the average of the two, thick lower curve, with the average difference between the residuals as a function of fit for each orientation of the substrate, bottom curve.

At this point it is worth noting that the residual as a function of fit for each orientation of the substrate are similar, even though the substrate is in a completely different orientation.

3.3 Creating a first-round calibration file: analysis description

The average of the residuals as a function of fit, over both orientations of the substrate, exhibits a high angular frequency fluctuation that is inspected in Fig. 9. The even order trend of the average difference between the residuals as a function of fit will be considered in section 5.4. The combined average was Gaussian filtered, with a radius of 12 points, to remove high angular frequency fluctuations which are most likely be artifacts of the mirror surface, and thus not applicable for a general calibration.

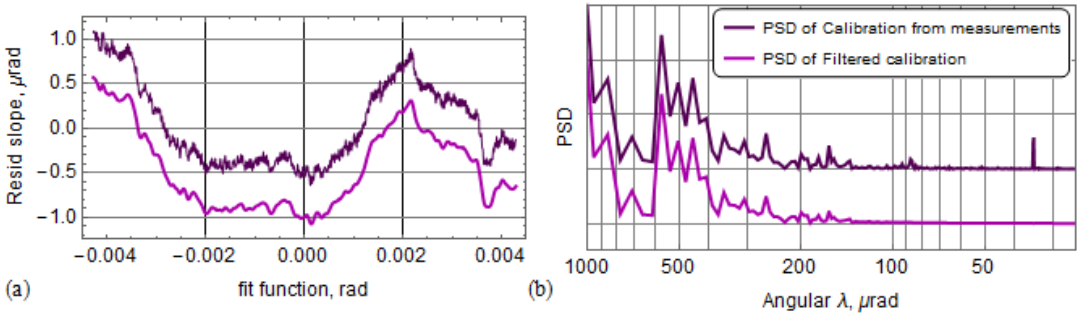

Figure 9: (a) The average residual as a function of fit, over both orientations of the substrate from raw data, upper curve, and with a Gaussian filter of 12 point radius, lower curve. (b) The associated PSDs

This filtered average residual slope as a function of best linear fit, with rms variation over the 8.5 mrad range of 0.457 μrad, may then be used as a first order calibration curve describing instrumental error that may be removed from measurements of curved optics. A refinement of this determined calibration will be examined in the next section.

3.4 Second round of calibration

In this section, the first-round calibration file, determined above, will be applied to each of the 32 prior measurements; each measurement within the eight regional trace pairs for each orientation of the substrate, direct and flipped, Fig. 10.

These calibrated measurements, Fig 10, will then be stitched together to give a determination of the mirror surface. To understand the error introduced by rotating and resampling slope data, for the purpose of stitching, we consider the rotation of a slope dataset that is itself a function of linear position

$$\begin{pmatrix} x_i \\ \alpha_{MES}(x_i) \end{pmatrix} \xrightarrow{Rot(\theta)} \begin{pmatrix} x_i' \\ \alpha'_{MES}(x_i') \end{pmatrix} = \begin{pmatrix} x_i\,Cos\theta - y_i(x_i)\,Sin\theta \\ ArcTan\left[\dfrac{Sin\theta + Cos\theta \cdot Tan\alpha_{MES}(x_i)}{Cos\theta - Sin\theta \cdot Tan\alpha_{MES}(x_i)}\right] \end{pmatrix}, \tag{2}$$

where the height distribution, $y_i(x_i)$, is given as a running sum of the measured slope

$$y_i(x_i) = \Delta x \cdot \sum_{x=0}^{x_i} Tan\,\alpha_{MES}(x_i) \tag{3}$$

and Δx is the increment of the measurements.

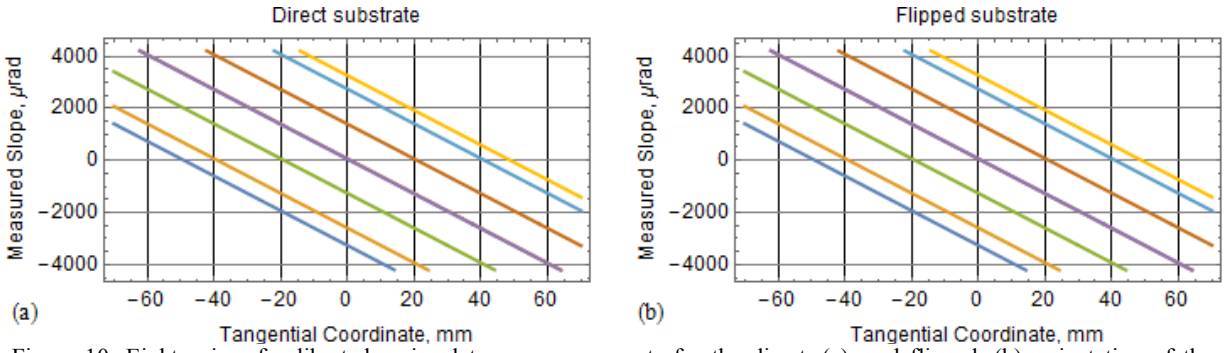

Figure 10: Eight pairs of calibrated regional trace measurements for the direct, (a), and flipped, (b), orientation of the substrate. Only seven traces are clearly visible as the central regional trace is repeated for each orientation. The negative slope progression does not mean that the SUT is convex, only that for the given arrangement of the pentaprism and autocollimator, the recorded angles have a negative trend. For ultimate measurement results, this is compensated for as a last step after all calibration is performed.

For the present purpose, the maximum rotation required for stitching, required for regional traces IV and VIII is less than 3.3 mrad, which for the spherical surface of the reference substrate will yield an introduced error as a function of position described with Fig. 11. The maximum error is introduced, 45 nrad at tangential position 20 mm, is a coordinate range common to all eight regional traces to be averaged. For tangential coordinates where the fewest, five, angularly overlapping measurements occur, the error is -25 nrad.

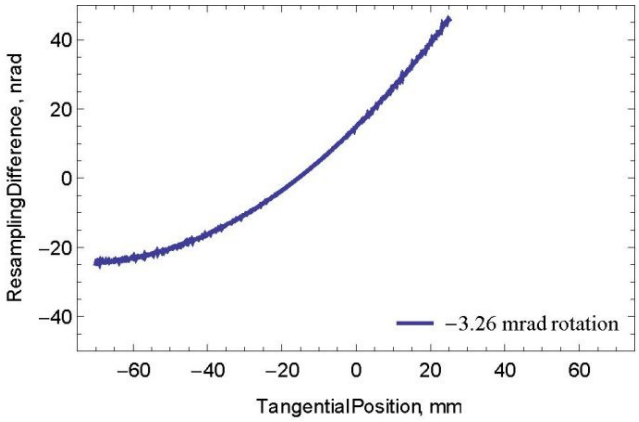

Figure 11: Plot of the error introduced by resampling rotated slope data for the purpose of stitching, for the case of the maximum rotation required, regional trace VIII.

As this resampling upon rotation error is 5 orders of magnitude less than the measurement range of ±4.5 mrad, and that this will be reduced upon averaging the common angular ranges, we are satisfied that we may reasonably trust the results of said stitching procedure.

This surface slope trace, determined from stitching the 16 pairs (eight direct and eight flipped) of calibrated measurements will then be subtracted from each calibrated measurement. The remaining residuals as a function of fit are again combined, as in section 5.2, in order to better compensate for the instrumental systematic error, Fig 12.

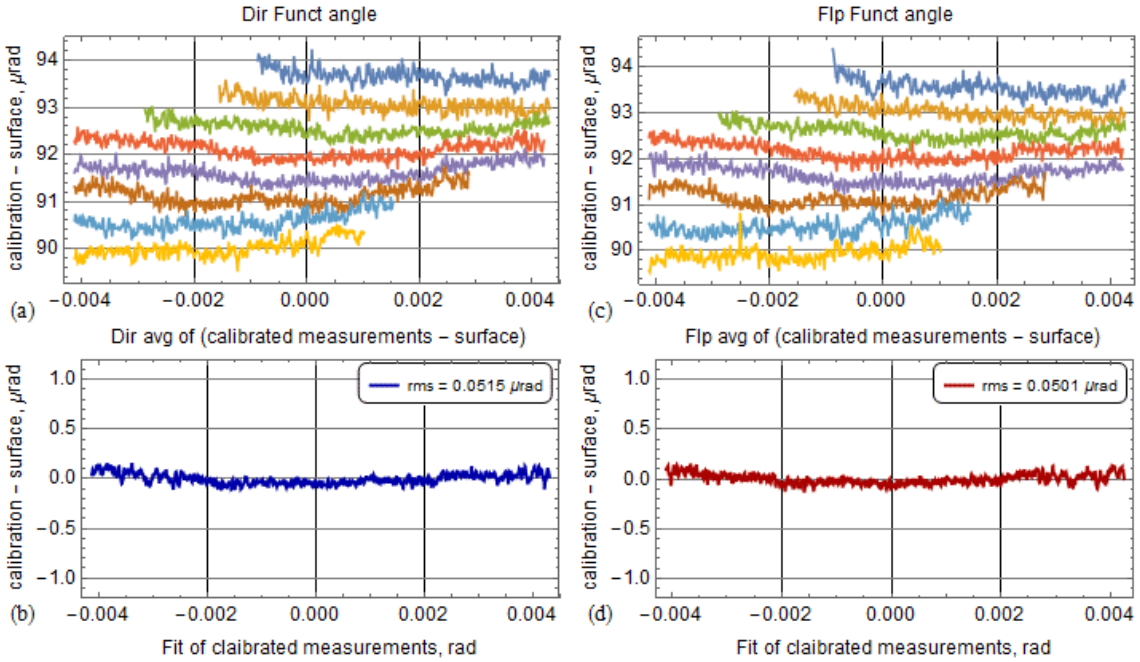

Figure 12: Top: Using the first round of calibration determined in Sec.5.3, the residual slope as a function of best linear fit of calibrated measurements, with the surface, determined from stitching, subtracted, for the direct (a) and flipped (c) orientations of the substrate (offset added for clarity). Bottom: The average over common domains with a zero order polynomial detrended for the direct, (b) and flipped (d) orientations.

Combining the above average residuals as a function of best linear fit of measurements with the surface subtracted, gives the second round of calibration that now accounts for the even order polynomial trend that was remaining after the first round of calibration, Fig 13.

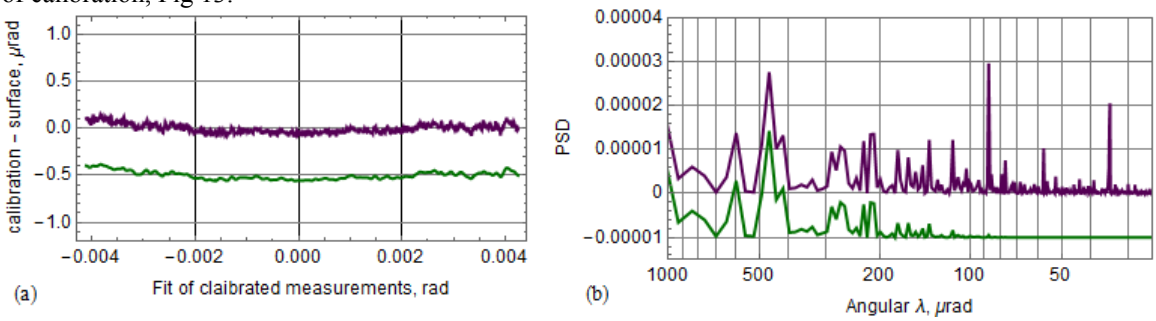

Figure 13: Average of the residuals as a function of linear fit of measurements with the stitched surface subtracted; raw data upper curve, Gaussian filtered with a 12 point radius, lower curve, (a). The associated PSDs, (b). This lower curve, filtered to remove surface artifacts, may be considered as the second round of calibration.

As a consideration to the efficacy of performing further calibration, we compare the results after the first two rounds, Fig. 14.

With a determination of the instrumental error added to measurements in hand, we may then subtract this calibration curve from measurements to obtain reasonable results of the surface shape of highly curved x-ray optics.

3.5 Considering the translational and time dependent stability of the DLTP

As a test of the translational stability of measurements, to check that the above determined calibration is valid, we performed a test where the substrate was translated upstream by 25 mm, and then downstream by 25 mm, with the results.

This net translational difference of 50 mm corresponds to approximately half, the anticorrelation, distance between the peaks of the residual slope trace found at roughly -40 mm and +60 mm from the substrate center. As there is no

discernable trend to the difference, we consider dividing this difference between the two measurements by the square root of two, to account for random noise, yielding translational stability on the order of 97 nrad rms.

For comparison, the time stability of measurements was also inspected, using the angularly centered regional trace pairs I and V, showing repeatability, with substrate repositioning, to be on the order of 84 nrad rms.

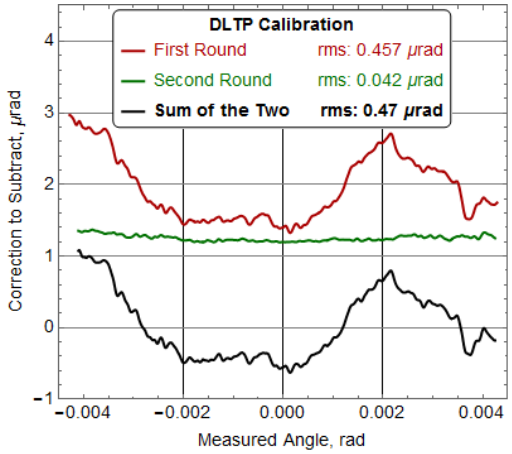

Figure 14. The results of two rounds of calibration data processing, bottom curve, as the additive sum of the first round, upper curve, and the second round, middle curve, of calibration data processing. We determine this sum to be a good representation of instrumental error added to measurements.

For a consideration of the actual translational variation, we may subtract in quadrature the translational stability from the time dependent instability and find the result to be 49 nrad rms. As this is an order of magnitude less than the calibration variance, we trust the calibration curve, over at least the central range of the DLTP translational carriage.

3.6 Utility of calibration information

With the calibration information in hand, highly accurate measurement results may be obtained with a fraction of the time otherwise required to reduce the impact of systematic error.[7] With the results of applying the calibration to a limited number of measurements, that may be carried out in a single day, produces nearly the same useful result as a carefully stitched, exhaustive series of measurements that may take, at best, 3 weeks to perform.

4. CONCLUSIONS

With an instrument optical table thermally stabilized to better than 2 mK rms, and the optimized air pressure, supplied to the DLTP translational carriage air bearings, we have demonstrated long term stability of the DLTP to be about 80 nrad rms for the main AC X-channel. This stability translates to 30 nrad rms stability of a typical scan run, consisting of 8 scans.

The repeatability test was carried out with a 180 mm super polished plane SUT. Comparison of two pairs of sequential measurement runs, each consisting of 16 scans, has confirmed the repeatability to be on the order of 26 nrad rms.

We have described a series of measurements and a system of data processing that was used to precisely calibrate the DLTP for measurements with significantly curved, 15 m spherical, reference mirror. The calibration has allowed us to measure 4 spherical substrates with radius of curvature about 19 and 29 meters with accuracy better than 80 nrad rms with speed improved by a factor of about 16.

In the course of the calibration experiments, we have characterized the surface residual slope variation of the reference mirror with accuracy better than 100 nrad rms. This mirror is now available for use as a calibrated standard helpful for fast and accurate calibrations of other profilometers.

In summary, we have demonstrated the capability of the DLTP, in the advanced environmental conditions in the new XROL, to provide fast, highly accurate surface slope metrology with error less than 40 nrad rms for flat, and less than 100 nrad for highly curved x-ray optics. This is a factor of three improvement compared to the DLTP performance prior to upgrade.

ACKNOWLEDGEMENT

The Advanced Light Source is supported by the Director, Office of Science, Office of Basic Energy Sciences, Material Science Division, of the U.S. Department of Energy under Contract No. DE-AC02-05CH11231 at Lawrence Berkeley National Laboratory.

REFERENCES

[1] Idir, M. and Yashchuk, V. V., Co-Chairs, "Optical and X-ray metrology," in [X-ray Optics for BES Light Source Facilities], Report of the Basic Energy Sciences Workshop on X-ray Optics for BES Light Source Facilities, D. Mills and H. Padmore, Co-Chairs, pp. 44-55, U.S. Department of Energy, Office of Science, Potomac, MD (March 27-29, 2013); http://science.energy.gov/~/media/bes/pdf/reports/files/BES_XRay_Optics_rpt.pdf.

[2] Takacs, P. Z., "X-ray optics metrology," in: [Handbook of Optics], 3rd ed., Vol. V, M. Bass, Ed., Chapter 46, McGraw-Hill, New York, (2009).

[3] Debler, E., Zander, K., "Ebenheitsmessung an optischen Planflächen mit Autokollimationsfernrohr und Pentagonprisma, PTB Mitteilungen Forschen + Prüfen," Amts und Mitteilungsblatt der Physikalisch Technischen Bundesanstalt, Braunschweig und Berlin, pp. 339-349, (1979).

[4] Siewert, F., Noll, T., Schlegel, T., Zeschke, T., and Lammert, H., "The Nanometer Optical Component Measuring machine: a new Sub-nm Topography Measuring Device for X-ray Optics at BESSY," AIP Conference Proceedings 705, American Institute of Physics, Mellville, NY, pp. 847-850 (2004).

[5] Lammert, H., Noll, T., Schlegel, T., Siewert, F., Zeschke, T., "Optisches Messverfahren und Präzisionsmessmaschine zur Ermittlung von Idealformabweichungen technisch polierter Oberflächen," Patent No.: DE 103 03 659 (28 July 2005).

[6] Siewert, F., Lammert, H., Zeschke, T., "The Nanometer Optical Component Measuring Machine;" Modern Developments in X-ray and Neutron Optics, Springer 2008.

[7] Geckeler, R.D., Weingärtner, I. , "Sub-nm topography measurement by deflectometry: flatness standard and wafer nanotopography," Proc. of SPIE, 4779, pp. 1-12, (2002).

[8] Geckeler, R.D., "Error minimization in high-accuracy scanning deflectometry," Proc. SPIE 6293, 62930O 1-12, (2006).

[9] Geckeler, Ralf D., "ESAD Shearing Deflectometry: Potentials for Synchrotron Beamline Metrology," Proc. of SPIE, 6317, (2006).

[10] Yashchuk, V. V., Barber, S., Domning, E. E., Kirschman, J. L., Morrison, G. Y., Smith, B. V., Siewert, F., Zeschke, T., Geckeler, R. and Just, A., "Sub-microradian surface slope metrology with the ALS Developmental Long Trace Profiler," Nucl. Instrum. and Methods A 616(2-3), 212-223 (2010).

[11] von Bieren, K., "Pencil beam interferometer for aspherical optical surfaces," Proc. SPIE 343, 101-108 (1982).

[12] Takacs, P., Qian, S. N., and Colbert, J., "Design of a long trace surface profiler," Proc. of SPIE, 749, pp. 59-64, (1987).

[13] Takacs, P., Qian, S. N., "Surface Profiling interferometer," US patent No.U4884697, Dec. 5, (1989).

[14] Qian, S., Jark, W., Takacs, Peter Z., "The penta-prism LTP: A long-trace-profiler with stationary optical head and moving penta prism," Rev. Sci. Instrum. 66 (3), 2562-2569(1995).

[15] Geckeler, R., Just, A., Krause, M. and Yashchuk, V. V., "Autocollimators for Deflectometry: Current Status and Future Progress," Nucl. Instr. and Meth. A, 616(2-3), 140-146 (2010)Geckeler, R.D., Weingärtner, I.., Just, A.., Probst, R.., "Use and traceable calibration of autocollimators for ultra-precise measurement of slope and topography," Proc. of SPIE, Vol. 4401, pp. 184-195, (2001).

[16] Just, A., Krause, M., Probst, R., and Wittekopf, R. , "Calibration of high-resolution electronic autocollimators against an angle comparator," Metrologia 40, 288-294 (2003).

[17] Yashchuk, V. V., "Positioning errors of pencil-beam interferometers for long-trace profilers," Proc. SPIE 6317, 63170A-12 (2006).

[18] Kirschman, J. L., Smith, B. V., Domning, E. E., Irick, S. C., MacDowell, A. A., McKinney, W. R., Morrison, G. Y., Smith, B. V., Warwick, T., and Yashchuk, V. V., "Flat-Field Calibration of CCD Detector for Long Trace Profilers," Proc. SPIE 6317, 67040J-11 (2007).

[19] Kirschman, J. L., Domning, E. E., Morrison, G. Y., Smith, B. V., Yashchuk, V. V., "Precision Tiltmeter as a Reference for Slope Measuring Instruments," Proc. SPIE 6317, 670409-12 (2007).
[20] Yashchuk, V. V., "Optimal measurement strategies for effective suppression of drift errors," Rev. Sci. Instrum. 80, 115101-10 (2009).
[21] Ali, Z., Artemiev, N. A., Cummings, C. L., Domning, E. E., Kelez, N., McKinney, W. R., Merthe, D. J., Morrison, G. Y., Smith, B. V. and Yashchuk, V. V., "Automated suppression of errors in LTP-II slope measurements with x-ray optics," Proc. SPIE 8141, 81410O-1-15 (2011).
[22] Yashchuk, V. V., Artemiev, N. A., Lacey, I., and Merthe, D. J., "Correlation analysis of surface slope metrology measurements of high quality x-ray optics," Proc. SPIE 8848, 88480I-1-15 (2013).
[23] Kirschman, J. L., Domning, E. E., McKinney, W. R., Morrison, G. Y., Smith, B. V. and Yashchuk, V. V., "Performance of the upgraded LTP-II at the ALS Optical Metrology Laboratory," Proc. SPIE 7077, 70770A/1-12 (2008).
[24] Artemiev, N. A., Merthe, D. J., Cocco, D., Kelez, N., McCarville, T. J., Pivovaroff, M. J., Rich, D. W., Turner, J. L., McKinney, W. R. and Yashchuk, V. V., "Cross comparison of surface slope and height optical metrology with a super-polished plane Si mirror," Proc. SPIE 8501, 850105-1-11 (2012).
[25] Irick, S. C., McKinney, W. R., Lunt, D. L., Takacs, P. Z., "Using a straightness reference in obtaining more accurate surface profiles from a long trace profiler (for synchrotron optics)," Rev. Sci. Instrum. 63(1), 1436-8 (1992).
[26] McKinney, W.R., Anders, M., Barber, S.K., Domning, E.E., Lou, Y., Morrison, G.Y., Salmassi, F., Smith, B.V., Yashchuk V.V., "Studies in optimal configuration of the LTP," Proc. SPIE 7801, 780106, (2010). V. V. Yashchuk, W. R. McKinney, T. Warwick, T. Noll, F. Siewert, T. Zeschke, and R. D. Geckeler, "Proposal for a Universal Test Mirror for Characterization of Slope Measuring Instruments," Proc. SPIE 6704, 67040A/1-12 (2007).
[27] Geckeler, R. D., "Optimal use of pentaprisms in highly accurate deflectometric scanning," Measurement and Science Technology 18, 115-125, (2007).
[28] Barber, S. K., Morrison, G. Y., Yashchuk, V. V., Gubarev, M. V., Geckeler, R. D., Buchheim, J., Siewert, F. and Zeschke, T., "Developmental long trace profiler using optimally aligned mirror based pentaprism," Opt. Eng. 50(5), 053601-1-10 (2011)
[29] Barber, S. K., Geckeler, R. D., Yashchuk, V. V., Gubarev, M. V., Buchheim, J., Siewert, F. and T. Zeschke, "Optimal alignment of mirror based pentaprism for scanning deflectometric devices," Opt. Eng. 50(7), 0073602-1-8 (2011).
[30] Elcomat 3000, Möller Wedel Optical, http://www.moeller-wedel-optical.com.
[31] Yashchuk, V. V., Artemiev, N. A., Lacey, I., McKinney, W. R. and Padmore, H. A., "A new x-ray optics laboratory (XROL) at the ALS: Mission, arrangement, metrology capabilities, performance, and future plans," Proc. SPIE 9206, 9206-13 (2014); this conference.
[32] Zafer, N., Luecke, G. R., "Stability of gas pressure regulators,"Appl. Mathematical Modelling 32, 61-82, (2008).
[33] Senba, Y., Kishimoto, H., Ohashi, H., Yumoto, H., Zeschke, T., Siewert, F., Goto, S., and Ishikawa, T., "Update of long ace profiler for characterization of high-precision x-ray mirrors at SPrint-8," Nucl. Instr. and Meth. A 616(2-3), 237-240 (2010).
[34] Probst, R., Wittekopf, R., Krause, M., Dangschat, H. and Ernst, A., "The new PTB angle comparator," Meas. Sci. Technol. 9, 1059 – 1066 (1998).
[35] Geckeler, R. D. and Just, A., "Optimized use and calibration of autocollimators in deflectometry," Proc. SPIE 6704, 670407-1 – 12 (2007).
[36] Geckeler, R. D. and Just, A., "Optimized use and calibration of autocollimators in deflectometry," Proc. SPIE 6704, 670407-1 – 12 (2007).
[37] Artemiev, N. A., Smith, B. V., Domning, E. E., Chow, K. P., Lacey,I., Yashchuk, V. V., "Angular calibration of surface slope measuring profilers with a bendable mirror," Proc. SPIE 9206, 9206-16 (2014); this conference.
[38] Polack, F., Thomasset, M., Brochet, S., Rommeveaux, A., "An LTP stitching procedure with compensation of instrument errors: Comparison of SOLEIL and ESRF results on strongly curved mirrors," Nucl. Instrum. and Methods A 616, 207-211, (2010).